XVI IMEKO World Congress
Measurement - Supports Science - Improves Technology - Protects Environment ... and Provides Employment - Now and in the Future
Vienna, AUSTRIA, 2000, September 25-28

TO PROBLEM OF MAGNETIC NON-DESTRUCTIVE TESTING

V. Setnicka, J. Bajcsy and M. Kollar*
Department of Measurement, *Department of Electromagnetic Theory
Slovak University of Technology
Ilkovicova 3, SK-812 19 Bratislava, Slovakia

Abstract: Many high quality Hall-type magnetic field sensors of advanced technology are customary available. We have experienced the use of Hall type sensors in non-destructive testing of material volume reduction due to corrosion and abrasion of iron tubes of different diameters as used for the heat exchangers, and gas pipelines.

Some results achieved by using a prototype assembly are presented. This consisted of a mechanical sensor moving support and a PC based measurement set for data recording and processing. Data gained are interpreted from the diagnosis point of view as the loss of ferromagnetic material and/or the thickness reduction. A program enabling to calculate distorted magnetic field has been developed with the aim to improve the design of sensor and to provide the measuring system with a sort of built-in intelligence for the evaluation of tests results.

Keywords: non-destructive testing, Hall probe, magnetic field solution

1 INTRODUCTION

Equipments as heat exchangers, steam generator tubes and pipelines are constructed from ferromagnetic materials (iron, steel). They are operating in aggressive environment and continuously are exposed to mechanical stress and/or the corrosion. Diameters of such tubes range from centimetres up to above one meter, and early detection of any defects is important not only from economical but also from environmental aspects. Besides other testing methods, based on the eddy-current effect from radio [1], to microwave frequencies [2], with different penetration depth, there is another possibility allowing for a spot excitation of tested pieces of material and therefore enabling to identify and localize the casualties. In fact, one can well use a static magnetic field - as caused *eg* by a permanent magnet. The local condition of material layer will be reflected via the changed stray field as the translational movement of the field source (permanent magnet) with respect to tested surface proceeds. This allows even for a relatively slow motion, if instead of induced voltage the magnetic field intensity (for instance by means of the Hall probe) will be sensed. On the other hand just contrary, the speed of this movement will be limited from above (by some eddy current considerations) to prevent one from a fuzzy interpretation of measured data. To make it clear, how the local conditions can influence this stray field, not only the experimental investigation but also some theoretical calculations are needed in order to implement results of both in a sophisticated testing equipment pro-viding it as well with an expert database as with recom-mendable decision-algorithms.

2 SENSOR AND TEST-SAMPLE

The magnetic sensor used in our experiments is in Figure 1. Inside a cap-like core, made from the soft magnetic material (outer and inner diameter 20 mm and 12 mm, height 20 mm) a cylindrical permanent magnet, with north and south poles as shown, was placed. At its bottom, the magnetic field intensity with the cap adjoined to a smooth uncorrupted magnetic surface was typically around 0.2 mT. When sliding along the tested surface, the static magnetic field intensity in the bottom air gap (approximately 1 mm) is continuously measured using *in*

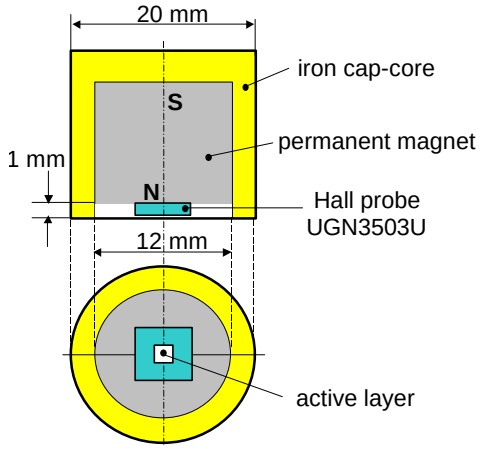

Figure 1. Magnetic field sensor construction

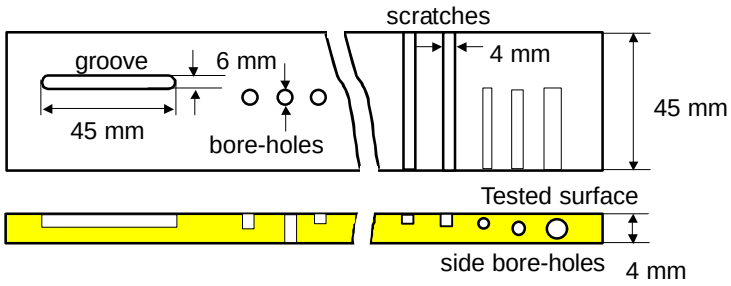

Figure 2. Testing bar with sample corruptions

situ placed active Hall probe of UGN3503U type with the output voltage directly proportional to the magnetic field intensity. Two different configurations were used, here referred to as *single* and *delta* sensor, with a simple or double Hall probe (connected in series opposition in the latter case).

An iron bar 600 mm in length, 45 mm wide and 4 mm thick, was intentionally corrupted by the bore-holes, grooves and scratches (see Figure 2) of different depth and orientation, to be used as a test-sample for checking the performance of the measuring equipment. In various tests, the intensity of the exciting magnetic fields was changed applying different types of permanent magnets. All the corruptions (2-6 mm) were of comparable or larger dimensions than the active layer (approximately 1x1 mm) of the sensor.

3 THEORY

Based on an assumption that the magnetic field in excited region (underlying the permanent magnet) causes homogenous magnetic polarization $\vec{\mathbf{J}}$ in a direction normal to the sample surface, one may expect the surface free poles developed at holes, scratches cavities and other irregularities to be sensed together with those appearing on the uncorrupted parts of the sample surface. According to Figure 3 a hole can be modelled by couples of charges having opposite signs. Fictive charges in the basal plane, which are positive, eliminate the fictive negative charges at the same spots, creating thus “the missing surface charges”, while the negative ones in the bottom are due to the discontinuity of normal components of magnetic polarization. In fact, all negative charges at the basal plane (including those which are only fictive) give rise to uniform field distribution and thus can be neglected. Since only the perpendicular-to-basal-plane magnetic field component activates the sensor, it can be concluded that not all poles will contribute while scanning the sample surface. Contributing are (i) poles at the basal plane located directly under the sensor active layer, (ii) "deepened" poles (*ie* developed at the irregularities) at all positions, including also poles not directly under the active layer. Fictive magnetic charges ΔQ_M, represented by charged surface elements ΔS, are proportional to the local normal component of magnetic polarization vector J_n. The density of surface magnetic charges s_M at the various types of irregularities may therefore vary considerably.

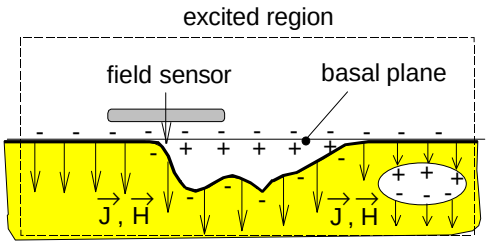

Figure 3. Excited region and the surface free poles as the stray-fields sources

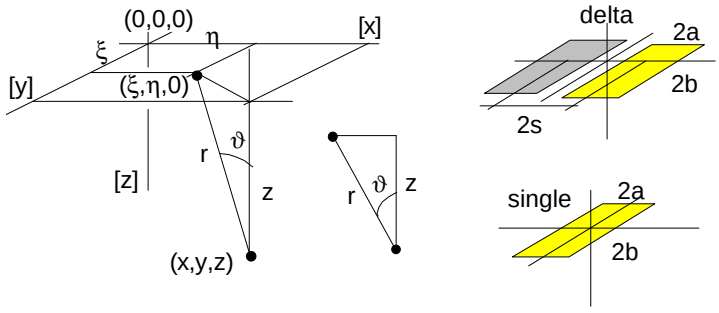

Figure 4. Relative position of the sensor active layer and stray-field point-source. The *single* and *delta* sensor configurations.

Let us suppose the magnetic polarization be proportional to the applied magnetic field intensity $\vec{\mathbf{J}}_n = -m_0(m_r - 1)\vec{\mathbf{H}}_n$, where m_r is the relative permeability of the sample. Since $s_M \equiv J_n$, the local magnetic charge assigned to an infinitesimal surface element ΔS is

$$\Delta Q_M(x,y,z) = s_M(x,y,z)\Delta S = -m_0(m_r - 1)H_n(x,y,z)\Delta S\,. \qquad (1)$$

In the case of a single sensor the voltage gained by the Hall probe is proportional to the magnetic flux integrated by its active layer (area 2*a*×2*b*) or to the *mean value* of the normal magnetic intensity field

component, while in a delta-sensor configuration this is given by the difference of the two appropriate (in opposite sense) integrated fluxes, see Figure 4.

The mean value of the normal magnetic field intensity component picked up by the sensor and caused by the poles at elementary surface ΔS of irregularity, can be estimated as

$$\langle \Delta H_\perp \rangle = \frac{1}{4ab} \int_\Sigma \Delta H_\perp \cdot ds \tag{2}$$

where Σ is the total sensor active area, in either case *ie* single or delta sensor configuration, and the (infinitesimal) contribution to the normal field given by

$$\Delta H_\perp = \frac{\Delta Q_M}{4\pi m_0} \frac{\cos\vartheta}{r^2} \quad \text{with} \quad r = \sqrt{(x-x)^2 + (y-h)^2 + z^2} \ . \tag{3}$$

In the case of a single layer sensor, using (2) to (4) we have for the absolute value of the mean magnetic field intensity

$$\left| \langle \Delta H_\perp \rangle \right| = \frac{s_M(x,y,z)}{2m_0} \cdot \frac{\Delta S}{S_0} \cdot z \iint\limits_{\substack{<-a,a> \\ <-b,b>}} \frac{dx\, dh}{\left[(x-x)^2 + (y-h)^2 + z^2 \right]^{3/2}} \tag{4}$$

where $S_0 = 4ab$ is the area of the active sensor layer. This after two-fold integration over the given region leads to

$$\left| \langle \Delta H_\perp \rangle \right| = \frac{s_M(x,y,z)}{2m_0} \frac{\Delta S}{S_0} \left[F(a,b) + F(-a,-b) - F(-a,b) - F(a,-b) \right], \tag{5}$$

where

$$F(a,b) = \frac{1}{2\pi} arctg \frac{(x+a)(y+b)}{z\sqrt{z^2 + (x+a)^2 + (y+b)^2}} \ .$$

The total sensed field is given by the integration of (5) wit possible use of (1) over the surface of all "excited" irregularities and over the uncorrupted part of the sample surface directly under the sensor active layer. Besides of all, the exact distribution of the surface charges is not known in advance and can be only, more or less precisely, estimated. This is, in general, very hard task and there-fore some simplifications have to be made. The latter integration will be hereafter replaced by a discrete summing of individual contributions according to (6), and the singular type of a *point* and *line* irregularities only will be considered. It is worth to notice that with $x = 0$, $y = 0$ and for $z \to 0$, it is $F(\pm a, \pm b) \to 1/4$, $F(\pm a, \mp b) \to -1/4$ then $h(a,b) \to 1$, and $|\langle \Delta H_\perp \rangle| \to s_M/(2m_0) \cdot \Delta S/S_0$, which even in the case of a charged surface element ΔS being represented just by one point charge ($Q_M = \sigma_M \Delta S$) located at its centre and in the active sensor layer plain ($z = 0$), gives the correct result $|\langle \Delta H_\perp \rangle| \to s_M/(2m_0)$, as $\Delta S \to S_0$. The last simplification, made for sake of briefness, does not impose serious restrictions to prospective irregularity shape and position inves-tigations as is, for example, the recognition and/or reconstruction from the sensed signal in an inverse task. In the case of these singular pole-sources (since they are dimensionless) the active layer of the sensor is still perceiving all underlying poles and the variable part of the stray field, which is only of interest, is due to the singular sources themselves. In fact, these sources may be considered as approximations based on averaged quantities in sense depicted in Figure 5 using more or less of them in a particular case. Both type of sensors were supposed to have a square active surface $a = b$, and the delta configuration to be edge-to-edge joint ($s = a$). In following figures

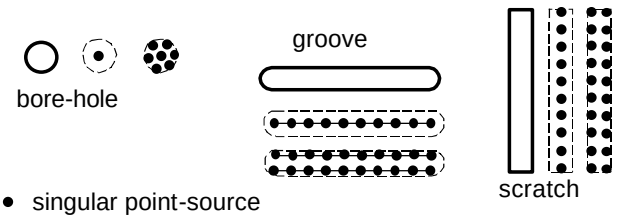

Figure 5. Corruptions and their equivalent (singular) sources

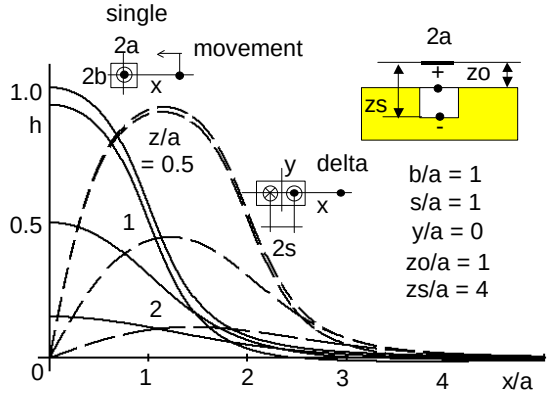

Figure 6. Hole-like corruption

there are given results of computations of a pair of point charges (a hole) and a pair of line charges (a scratch or groove) passing under the both type of sensors (single and delta) at a considerably low velocity. In every picture the curves at the left (full line) belong to *single sensor*, whilst those at right (dashed lines) were calculated for *delta sensor* configuration. In the case of *delta* sensor, to evaluate $\langle H_\perp \rangle$ two consecutive shifts by $\pm s$ in a numerical procedure according to (6) were used. In all pictures below a reduced (dimensionless) value of the magnetic field intensity h is shown instead of $\langle H_\perp \rangle$ so that the maximum value is always unity, but the shape and relative magnitudes of particular instances are preserved. In fact these values should by added to a (negative) "background" caused by, in ideal case evenly distributed, surface poles at the basal plane. For simplicity, this background caused by negative poles on uncorrupted parts of the sample surface and the fictive negative poles (see Figure3 for details) was not taken into account.

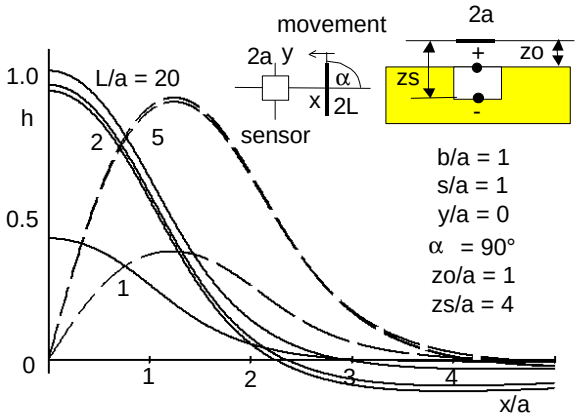

Figure 7. Scratch-like corruption

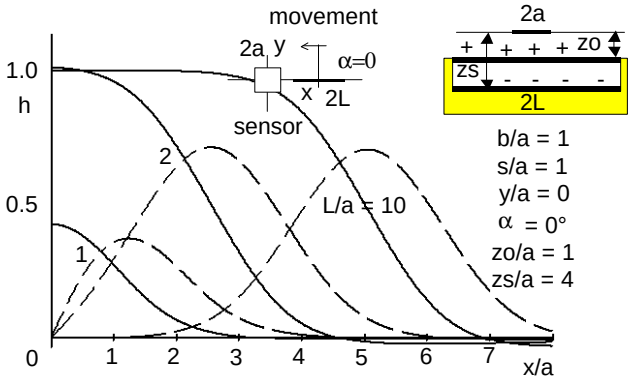

Figure 8. Groove-like corruption

The line-pole source was replaced by a chain of point sources with a number being proportional to the line (scratch or groove) length, typically counting as much as tens of points on a length of *a*. The sensitivity to the distance from the active sensor layer, if the displacement occurs along the line going through the centre of the hole, is shown in Figure 6. It is clear that the deeper are the source-poles the smaller voltage can be gained. The voltage sensed in the case of a line with variable length (2*L*) declined at angles $\alpha = 90°$ (scratch) and 0° (groove) from the direction of its translational movement are in Figure7 and Figure8. The sample surface under the tests was typically as close to the sensor active layer as *zo*/*a* = 1 and the depth of the corruptions in all shown cases was estimated to *zs*/*a* = 4, which was approximately the half- thickness of the testing bar. The coordinate *y* relates the centres of the considered singular sources. Finally, an estimation of cavity was conducted using the same numerical procedure. The idea is depicted in the right part of Figure 3, and is based on that poles of opposite signs are developed at the upper and lower surfaces of the immersed cavity. Result of evaluation for this case is shown in Figure 9. This, a bit dangerous treatment – since between the discretely spaced sources one will always find a rippling component – ma be justified by a supposition of more complicated flux distribution around such a cavity. How much is this close to a real case would anyhow require more investigation. However, similar but much more picturesque course of the voltage was recorded on a relatively large side bore-hole, nearly 4 mm in diameter, in a 4 mm thick test-bar. It should be noted that detecting of smaller cavities on the other hand is difficult due to a low level of the gained signal. Here presented calculations may be extended to some more complicated structures in general. The code allowing for a multiple use of randomly distributed singular sources, used to describe eventual corruptions, has been written, and found to operate satisfactorily.

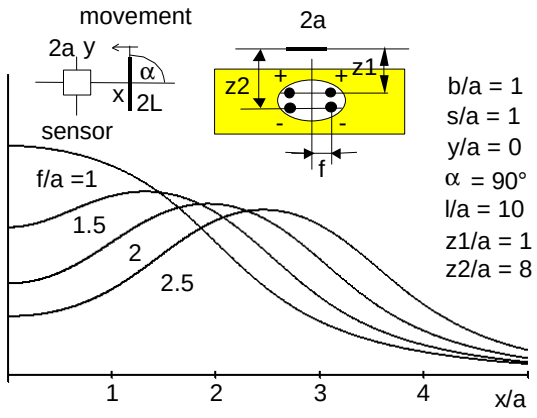

Figure 9. Side-hole-like corruption (cavity)

4 EXPERIMENTS

Several experiments were performed. In most of them the sensor (single or delta) was moved along the disturbance at a relatively slow speed (typically 1mm/sec) at which no time dependent effects were believed to influence the result of measurements. The sensor relative position was recorded in mm and the field intensity (the observed voltage is shown in the figures at the vertical axes) only in relative units, since the gain of the sensing loop was adjustable in a wide range.

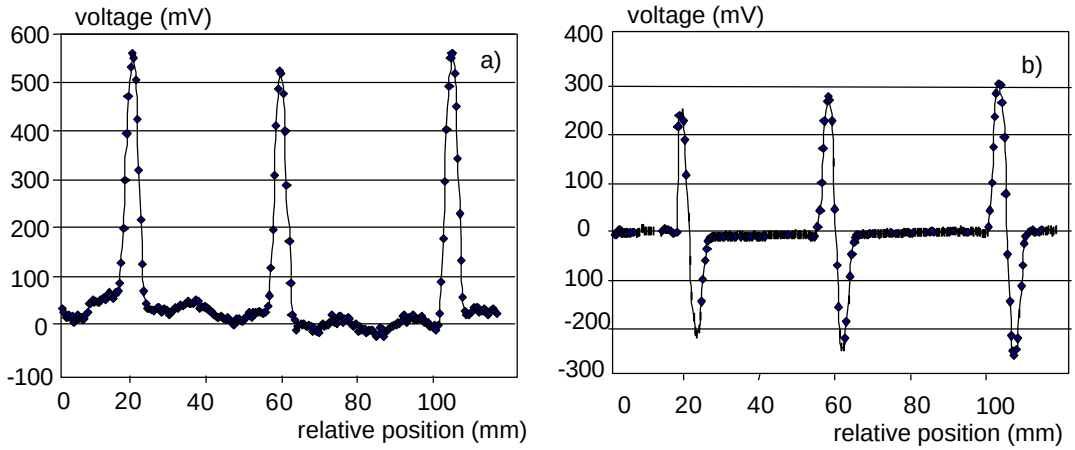

Figure 10. Bore-holes: a) single sensor, b) delta sensor

In Figure 10 there are results of a measurement at a group of three boreholes of slightly different size and depth and of unequal displacement as sensed by both the single- and delta-sensors. This should be compared with the evaluation result shown in Figure 6. In Figure 11 the results on a pair of perpendicular-to-movement scratches of different depth is shown, and Figure 12 shows essentially the same for a groove with longitudinal-to-movement orientation. The evaluated shapes are shown in Figure 7 and Figure 8, respectively.

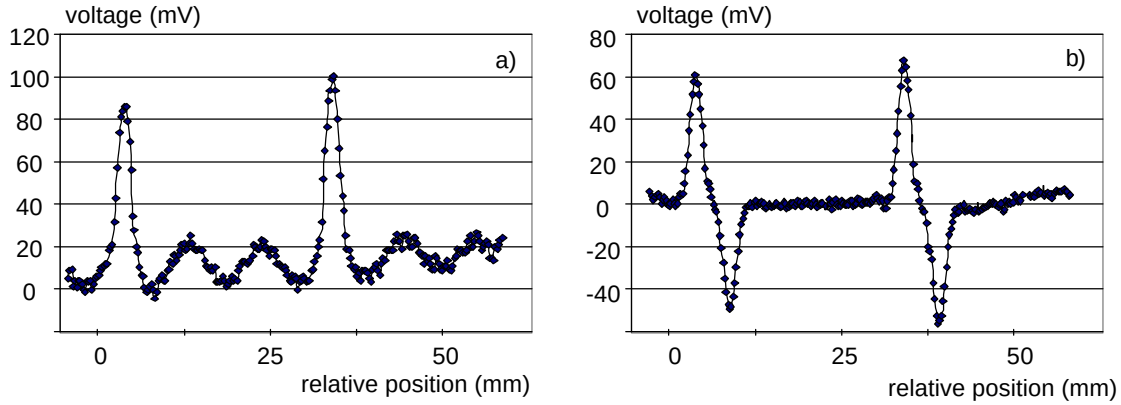

Figure 11. Scratches: a) single sensor, b) delta sensor

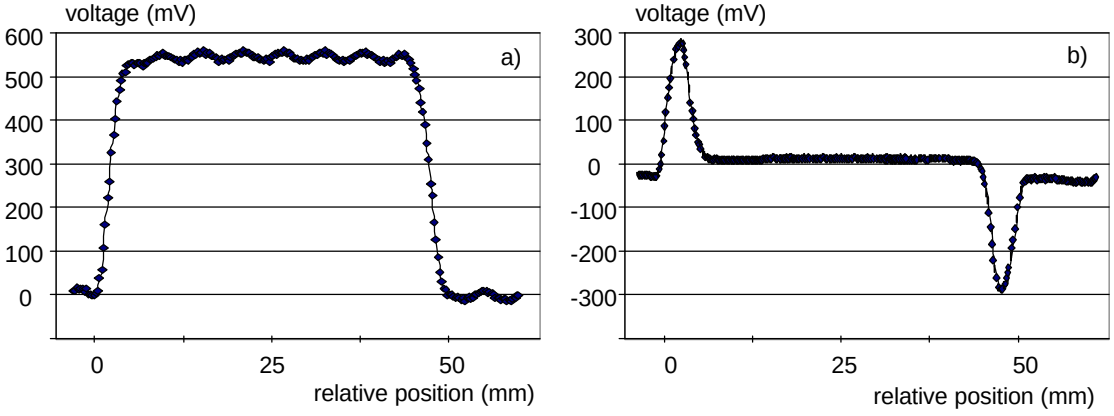

Figure 12. Groove: a) single sensor, b) delta sensor

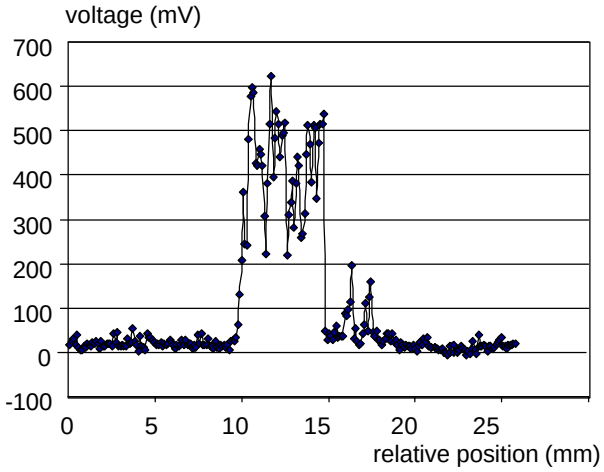

Figure 13. Side-bore-hole - single sensor

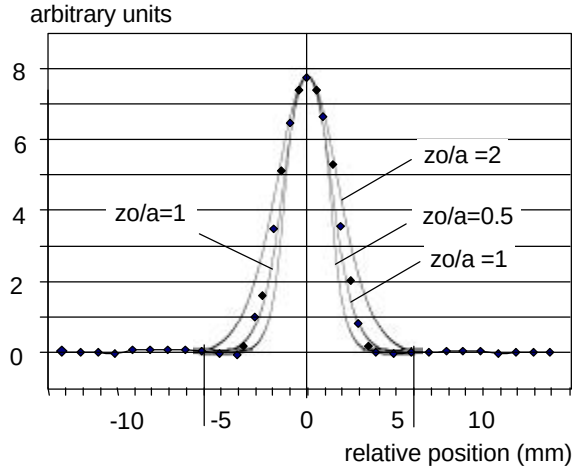

Figure 14. Bore-hole, diameter 6 mm, step 0.5 mm - as sensed by a single sensor

The case of a pair of side-bore-holes (cavities) is in Figure 13, and its evaluation can be found in Figure 9.

5 DISCUSSION

In Figure 14 there are compared the voltages at a bore-hole as measured and calculated using above theory – a pair of single point charges as an equivalent (singular) source. The height of the "pulse" was fitted to the same value and the shape, depending on the distance of the sensor from the basal plane, is displayed. If one estimates the active layer of the sensor be in the middle of about 1 mm thick Hall probe element case and its linear dimensions are said to be $2a$ = 1 mm, then, considering its separation from the basal plane to be approximately 0.5 mm one gets $z_o/a = 1$. Processing of the appropriate shapes from Figure 6, as depicted in Figure 14, has led to a good agreement.

Unlike in the cases of a hole, scratch or a groove (Figure 10 to Figure 12) where all the main features are clearly seen, the cavity (Figure 13), formed here as a side bore-hole, seems to be somewhat troublesome. This can be attributed to perhaps more complicated magnetic flux in the vicinity of such a corruption, tending to form a closed path instead of the simpler distribution anticipated in our considerations.

6 CONCLUSION

It has been shown that a reliable distinction between different types of possible corruptions of the iron tubes is possible, using a simple technique based on the permanent magnet excitation and a Hall probe detector used to test the local stage of material. The fundamen-tal importance of such measurements lies in early diagnostics of the technological conditions of various supply lines. Particularly it is worth to mention that the method is non-destructive, and it is suitable for the testing of ferromagnetic materials. Experimental results corresponded well with the theoretical prediction concerning the magnetic field shape in the vicinity of considered type of defects.

This method, although based on the static field measurement, could be perhaps used also in conjunction with faster moving measuring equipment, if it will be proved that the operating velocity substantially does not deteriorate the data gained in static or a slow-movement case.

REFERENCES

[1] Bajcsy, J.; Ravas, R.; Setnicka, V.; Smiesko, V.: To the sensitivity of a defectoscopic device measuring probe, Journal of Electrical Engineering, Vol. 46, 1995
[2] Kollar, M.; Franek J.; Kabos, P.: Microwave Resonator for Microwave Nondestructive Testing, Journal of Electrical Engineering vol. 50 (1999) No. 8/s, 82-85

AUTORS: V. SETNICKA and J. BAJCSY, Department of Measurement; M. KOLLAR, Department of Electromagnetic Theory, Slovak University of Technology, Faculty of Electrical Engineering and Information Technology, Ilkovicova 3, 812 19 Bratislava, Slovakia, Phone / Fax: ++ 421 7 654 29 600, E-mail: julo@pluto.elf.stuba.sk